This is a preprint, the final version is subject to change, of the American Mineralogist (MSA)
Cite as Authors (Year) Title. American Mineralogist, in press.
(DOI will not work until issue is live.) DOI: http://dx.doi.org/10.2138/am.2013.4249

Revision 1

Geometric analysis of radiation damage connectivity in zircon, and its implications for helium diffusion

Richard A. Ketcham[1], William R. Guenthner[2], Peter W. Reiners[2]

[1] Jackson School of Geosciences, The University of Texas at Austin, Austin, TX, USA

[2] Department of Geosciences, University of Arizona, Tucson, AZ, USA

Keywords: zircon, radiation damage, percolation, alpha recoil, fission track, diffusivity

Abstract

Geometrical modeling of radiation damage zones from alpha recoil and fission that accounts for their elongate nature provides new estimates of the doses required to reach percolation and full connectivity in zircon. Alpha recoil track damage percolates at doses from 2.5-3.1 x 10^{16} α/g based on our calculations, about two orders of magnitude lower than previous estimates, with the difference partially due to elongation and partially due to decay chains creating pre-made networks of connected tracks. This dose level is far below that required for metamictization, and suggests that alpha recoil track percolation has no effect on macroscopic or unit cell properties, at least as measured to date. However, fission tracks percolate at a dose of approximately 1.9 x 10^{19} α/g, the approximate level formerly ascribed to alpha recoil damage percolation and correlating with various transitions in material properties, such as an inflection in the relationship between dose and macroscopic swelling. Consideration of the undamaged regions between damage zones indicates that c-axis-parallel channels are frequently interrupted, at the μm scale at very low doses and 10's of nm at usual doses in natural zircon, with the

probable effect of decreasing diffusivity anisotropy. The percolation and further interconnectivity of alpha recoil damage corresponds with a general minimum in diffusivity and maximum in closure temperature in zircon, indicating that alpha recoil damage percolation does not make a grain "leaky", but instead quite the opposite. Instead, the onset of poor He retentivity at high damage levels correlates with fission-track percolation. Some of these results are non-intuitive with respect to the trapping model of He diffusivity reduction, and the alternative mechanism of tortuosity is discussed.

Keywords: zircon, percolation, alpha recoil, fission track, diffusivity

Introduction

Radiation damage is known to exert a strong effect on helium diffusivity in apatite and zircon (Holland, 1954; Holland and Gottfried, 1955; Hurley, 1954; Hurley et al., 1956; Nasdala et al., 2004; Nasdala et al., 2001; Reiners, 2005; Shuster et al., 2006). At low overall damage levels ($<10^{17}$ α/g) in both natural and synthetic apatite, diffusivity decreases with increasing radiation damage (Shuster and Farley, 2009; Shuster et al., 2006). Farley (2007) postulated that low He retentivity in synthetic zircon-structure minerals compared with natural zircon may be due to lack of radiation damage. Although radiation damage effects on helium diffusivity in apatite are well-characterized, zircon presents additional challenges because the higher characteristic amounts of U and Th generate damage sufficient to lead to metamictization on geological time scales. This in turn has been postulated to be responsible for high helium diffusivity and young (U-Th)/He ages that are poorly reproducible but well-correlated with U-Th content and thus damage (Hurley, 1954; Reiners, 2005).

The primary source of radiation damage in U-Th-bearing minerals is alpha recoil. Although alpha particles carry more energy, they do not interact as destructively with the crystal structure (Holland and Gottfried, 1955), and can even promote annealing in some cases (Ouchani et al. 1997). Fission tracks are individually much more destructive, but they are also far less abundant; for ^{238}U, alpha recoils are about 1.76×10^7 more abundant than fission decays, and ^{232}Th does not undergo spontaneous fission. Overall, approximately 10^5 times more kinetic energy is deposited into the crystal structure by alpha recoil than by spontaneous fission (Shuster and Farley, 2009). For this reason the effect of fission damage on zircon structure and properties has previously received relatively little attention.

At low levels of radiation damage, alpha recoil damage zones have been theorized to constitute isolated "traps" which He has difficulty escaping from, lowering overall diffusivity (Farley, 2000). However, as radiation damage levels rise, and an increasing fraction of the crystal structure becomes damaged, the damaged zones may begin to interconnect. Once there is a fully connected path through the solid, a state known as "percolation" is achieved.

Percolation of radiation damage is thought to influence various aspects of material behavior; Ewing et al. (2003) cite a number of possible ramifications of percolation relevant to zircon. Percolation may be partially or wholly responsible for a change in macroscopic swelling behavior as a function of dose (Trachenko et al., 2000; Trachenko et al., 2003) and in the relationship between macroscopic swelling and unit cell expansion (Ríos et al., 2000; Salje et al., 1999). In addition, it may be expected to cause changes in dissolution and transport properties of minerals (Jonckheere and Gögen, 2001) for various species (He, Pb, etc.).

Percolation theory is well known in mathematics (Hunt and Ewing, 2009, and references therein). It is most commonly described in terms of the connectivity of grids or lattices (Fig. 1). If one takes a grid of points, and begins randomly connecting neighboring points with vertical and horizontal line segments, as the proportion of possible links made (p) rises, clusters of connected links begin to form; the proportion of links connected the largest cluster is termed P_{max}. Eventually a threshold is surpassed at which a connected network forms that extends from the top to the bottom of the grid. Importantly, and perhaps non-intuitively, this critical percolation threshold (p_c) is independent of the grid extent; no matter how large the grid is, once p_c is surpassed a network extends to its boundaries. The percolating network of links is thus termed the infinite cluster, as it would extend infinitely in all directions in an infinite grid. Although infinite in extent, however, it does not necessarily encompass all of the connections that were made, and the proportion of links connected to the infinite cluster is termed P_∞; the infinite cluster is always the largest, and so P_∞ and P_{max} are equivalent once percolation sets in. As more links are added and p continues to rise, eventually all links will be connected to the infinite cluster and P_∞ will approach unity.

Although percolation is most easily portrayed and calculated using grids, the concept also extends to continua, in which case p and p_c represent the volume fraction of the percolating phase (i.e. damage tracks), and P_{max} and P_∞ are the proportion of tracks connected to the largest and infinite cluster, respectively. In comparison to work on radiation damage in zircon, p corresponds to the amorphous fraction (f_a) under the direct-impact model in which each decay event is sufficient to form amorphous material (Gibbons, 1972):

$$f_a = 1 - e^{-B_a D}, \quad (1)$$

where B_a is the mass of amorphous material produced per decay, and D is dose. In the zircon literature f_a corresponds exclusively to the damage caused by alpha recoil, because of the relatively minor contributions of other damage types. In this work we will use the variable p rather than f_a, to maintain consistency with the percolation literature, and also to more easily generalize the discussion to include fission damage without confusion.

Trachenko et al. (2000) used a grid-type approach to model damage zones in zircon as basically equidimensional, and obtained a p_c value for the amorphous volume fraction of 0.316, similar to the percolation values for a cubic grid (0.312; Fig. 1). However, percolation is strongly affected when the structures under consideration are elongated. Garboczi et al. (1995) demonstrated for ellipsoids of revolution (ellipsoids with two equal axes equal) that, as elongation increases, the number or volume fraction of structures necessary for percolation decreases. For example, for an aspect ratio of 1 (i.e. spheres) p_c is 0.287, similar to a square grid, whereas for an aspect ratio of 10 p_c is 0.087, and if the aspect ratio is 100 it falls to 0.0069. Insofar as both alpha recoil and fission produce strongly elongated damage zones, the percolation behavior of this damage in zircon merits reconsideration.

Radiation damage dimensions

To model percolation, one first needs a simple geometrical model for the percolating phase. Accordingly, the modeling in this paper is solely concerned with the principal damage zone caused by a recoil nucleus or fission pair, and not with secondary features such as cascades that branch from the main damage body, or point defects caused by propagation of strain through the matrix. Molecular dynamic (MD) modeling by Devanathan et al. (2006) for low-energy

alpha recoils suggests a roughly cylindrical amorphous core, reflecting a consistent rate of energy loss for the recoil nucleus along its trajectory.

Alpha recoils resulting from natural decay of U and Th have energies from 70-140 keV, with the mean value being close to 95 keV for both the ^{238}U and ^{232}Th decay chains. The range for a 95 keV massive nucleus along the U-Pb decay chain in zircon predicted by SRIM (Stopping and Range of Ions in Matter; Ziegler et al., 2008) is approximately 25 nm. For reasons of simplicity, in this study all recoil tracks are given a 25 nm length, neglecting the variation caused both by differing recoil energies and by straggling (e.g., Jonckheere and Gögen, 2001), which we assume will have at most a second-order effect on the calculations here.

The diameter of an individual alpha recoil damage zone is difficult to measure, but transmission electron microscope (TEM) imaging of alpha recoil tracks by Weber et al. (1994) suggests that the damage diameter is on the order of 2-5 nm, with some isolated elongated zones supporting the lower end of this range. Molecular dynamics (MD) modeling of 10 keV and 30 keV recoils (Devanathan et al., 2006) result in an amorphous core with a diameter of 2-2.5 nm. Unfortunately, the long range of recoil nuclei at the high energies characteristic of the U and Th decay chains substantially increases the computational burden of modeling them, and we know of no MD studies that approach recoil energies of 95 keV. An estimate of damage radius can also be obtained by taking an estimate of the mean amount of damage formed by a single recoil (5.48×10^{-19} g/α-event; Palenik et al., 2003), and casting it as a cylinder of length 25 nm. The resulting diameter is 2.44 nm, very much in line with the TEM and MD results.

The picture of the principal component of an alpha recoil track damage zone as resembling an elongated cylinder may be an unaccustomed one, as some previous rough

portrayals of recoil damage connectivity and percolation suggest a spherical damage zone (e.g., Gögen and Wagner, 2000; Trachenko et al., 2003). Similarly, some MD models also appear to generate a more equant zone (e.g., Trachenko et al., 2002), although it should be recognized that these are of low-energy recoils with short stopping distances, and moreover that in many simulations the recoil has a plunge angle making its track appear shorter when viewed orthogonal to the simulation lattice. If one accepts the SRIM-estimated stopping distance as reasonable, however, the conclusion of a highly elongated zone is unavoidable.

Fission tracks present a considerably more severe instance of elongation. The stopping distance of the pair of fragments from spontaneous fission in zircon is 16.7 μm (Jonckheere, 2003; Ziegler et al., 2008), and the diameter of the damaged zone, as imaged by TEM, is 5.4 nm (Lang et al., 2008).

Connectivity modeling

Motivation

The principal study of the percolation of elongated regions was conducted by Garboczi et al. (1995), who computationally modeled ellipsoids of revolution with various aspect ratios, by randomly placing them into a volume and determining when the upper and lower boundaries of the volume were intersected by a single cluster of connected objects.

Based on the dimensional considerations discussed above, alpha recoil tracks are estimated in this work as having a long axis/short axis ratio of about 10, which for the case of ellipsoids of revolution is predicted to result in percolation at a volume fraction of 0.087 (Garboczi et al., 1995). The considerably more severe elongation of fission tracks (long axis/short axis ≈ 3000) exceeds the range evaluated by Garboczi et al. (1995), although it is

within a reasonable range of extrapolation from their results, which predict formation of a percolation network when their volume fraction is approximately 0.0002.

The techniques employed by Garboczi et al. (1995) provide the starting point for this study, but a number of details of the natural systems being studied, and the problems being considered, required a new treatment.

First, rather than being fully random, natural alpha recoils occur in chains of 8, 7, or 6, depending on the original parent isotope (^{238}U, ^{235}U, ^{232}Th). The recoil damage zones originating from a single parent are certainly clustered together, and they are very likely to be interconnected. MD modeling indicates that the recoiling nucleus comes to rest within the damage zone, and thus it will be connected to the damage caused by its next alpha recoil. The assumption of connectivity is broadly supported by the success of alpha recoil track dating (Gögen and Wagner, 2000; Jonckheere and Gögen, 2001).

Second, MD modeling suggests that the shape of the damage zone from alpha recoil is probably closer to a cylinder than an ellipsoid of revolution. The correct choice for a fission damage zone is less clear, as annealing of tracks as revealed by etching suggests a central zone of uniform diameter that tapers off toward the track ends (Carlson, 1990), but TEM data may indicate a more steady decrease from track center to tip (Li et al., 2012).

Third, we wish to extend our analysis past the percolation threshold to also examine the onset of massive connectivity, when virtually all damage zones are connected (i.e. P_∞ approaches 1.0), as this could be expected to influence helium diffusion.

Fourth, we also wish to extend our analysis to examine the geometric properties of the regions not affected by radiation damage. In particular we wish to examine the continuity of the

undamaged regions between tracks, and whether these regions have a characteristic dimension, and how this dimension may relate to He diffusivity.

Implementation

The primitive object used to represent the radiation damage zone in this study is a "capsule", which is defined by the set of points that are within a certain radius of a line segment (Fig. 2a); it is essentially a cylinder capped with a half-sphere at each end. This shape was chosen over a cylinder because it enables a very efficient test for intersection between two tracks, consisting of determining whether the shortest distance between the two line segments is less than the sum of the radii. To generate a capsule representation of a track, a line segment with a random orientation is generated with the length of the damage zone in question, and then the endpoints are offset inwards by the track radius. To account for the slightly smaller volume of a capsule as compared to a cylinder of equivalent length, the radius of alpha recoil tracks is increased from 1.22 nm to 1.239 nm so the total volume remains 5.48×10^{-19} g/α (Palenik et al., 2003). For fission tracks, the length and radius discussed previously are used directly.

For the purposes of this study, connectivity is solely a function of whether damage zones intersect, without regard to the material properties of the tracks, or whether they vary radially or along their lengths. Until doses exceed amounts linked with macroscopic swelling ($>10^{18}$ α/g), we expect these zones to be amorphous, but with average density similar to undamaged zircon, as any volume increase would have to be accommodated as strain in the surrounding material. According to the direct impact model (Palenik et al., 2003), even at a dose of 4×10^{17} α/g, where there is no sign of swelling, the amorphous fraction is 20%. We also omit annealing, assuming

that all tracks retain their initial geometry; this simplification is common for zircon, as annealing of recoil damage probably negligible at near-surface conditions (Nasdala et al., 2001).

To study percolation and interconnectivity, it is not necessary to model the entire mineral grain, which would be out of the question for alpha recoil tracks in a typical zircon crystal because their number would overwhelm computer resources. For example, a 100-μm cube with 10^{17} α/g (e.g., a zircon with U=272 ppm, Th/U=0.5, and age=100 Ma, resulting in 166 nmol He/g) would have 470 billion alpha recoil tracks. Fortunately, a representative volume that sufficiently exceeds the length of the longest damage axis is sufficient to test for percolation. To study alpha recoil track connectivity, we used cubic representative volumes of 1-2 μm on a side (1-8 μm^3), and verified that our volume was representative by comparing results for volumes of different sizes. Because of their much greater length, for fission track connectivity we were forced to model much larger volumes of 170-200 μm on a side, approaching the size of a typical crystal used for thermochronology. Recoil and fission damage were modeled separately.

The first computational step is to create the tracks, by generating a random endpoint in the model space followed by an orientation vector defined by a random azimuth ϕ in $[0,2\pi]$ and inclination ψ in $[-\pi/2, +\pi/2]$, the latter generated by taking the arcsine of a uniform variable in the interval [-1,1]. The second endpoint is determined by the track length and the orientation vector. Connectivity of recoil tracks in chains was modeled by using the second endpoint of a track for the first endpoint of the next (Fig. 2b); chains of 8 for ^{238}U and 6 for ^{232}Th were modeled, as well as 1 (i.e. independent tracks) for comparison. Tracks were allowed to intersect the boundary of the volume, but if a track in a chain did so, the chain was truncated at that point. Each track is given a boundary code reflecting which of the six model space boundaries it intersects, if any.

The next step is to test the tracks for intersection. To increase the efficiency of this step, we utilize the approach of Garboczi et al. (1995) by first subdividing the calculation volume into smaller cubic elements and pre-calculating which damage trails intersect which elements. This allows testing only the sets of tracks within each sub-volume for intersection, greatly increasing the efficiency of the algorithm.

A set of intersecting tracks is classified as a cluster. Each track is assigned a cluster code, denoting which cluster it is in, if any. As intersection testing continues, clusters are formed and merged as more intersections are found. Contact of clusters with the boundaries of the model space is determined by merging the boundary codes of each of the tracks within it. Percolation is considered fully achieved when a single cluster intersects all six boundaries of the model space. This is a slightly stronger percolation condition than used by Garboczi et al. (1995), who only considered intersection with two opposing surfaces; the effect is to move the percolation threshold to a slightly larger value, but make it more reproducible in the face of the stochastic nature of track generation.

The character of the space between alpha tracks is evaluated in two ways (Fig. 3). The first is the Mean Intercept Length (MIL) test, in which the spacing between alpha recoil or fission tracks in the volume is characterized by projecting lines through the model space at random locations and counting the number of tracks intersected. The line length divided by the number of intersections determines the mean intercept length (l_{int}). Thus the MIL test quantifies the average distance a particle can travel in a single direction without encountering a damage zone. In addition, by analogy with packed spheres, l_{int} can be considered as the radius of the interior zones unaffected by the radiation damage in question, and is thus a candidate for a

characteristic length-scale for the interruption of undamaged material, which may in turn be taken as a gauge of the tortuosity of region occupied by undamaged material.

Because the zones of undamaged crystal are very irregular, another calculation was made of the mean distance from a randomly-placed point in undamaged crystal to the nearest track (d_n). If we consider the edge of a damage zone to be a potential boundary to a domain of fast material transport (provided interconnection of damage zones allows fast transport out of the grain.), we can use this as an possible estimate of the characteristic length scale for diffusion in undamaged material. Values for d_n for the canonical geometries of spheres, infinite cylinders, and infinite sheets, are $r/4$, $r/3$, and $t/2$, respectively, where r is radius and t is half-thickness.

Results

Modeling results for alpha recoil tracks with chain-lengths of 8, 6, and 1 respectively are provided in Tables 1-3, and Table 4 reports results for fission tracks. In sensitivity testing, it was found that the p_c, l_{int}, and d_n are not sensitive to the volume of the space being modeled. However, P_{max} tends to have smaller values in smaller volumes, reflecting an artificial boundary effect: smaller volumes have larger surface to volume ratios, and tracks and clusters near a model boundary are more likely to escape being intersected by the infinite cluster. Unfortunately, limitations in computer resources prevented the total eradication of this effect, but it is minimized in the case of 8-length alpha recoil track chains and fission tracks. The results for connectivity are discussed first, followed by those for the undamaged volume.

Connectivity

For 8-length alpha recoil track chains, the percolation threshold is reached at a dose of approximately 2.5×10^{16} α/g. Massive interconnectivity sets in fairly quickly afterwards with

over 95% of tracks connected in a single cluster at about 5.3 x 10^{16} α/g. 6-length chains reach percolation at a slightly higher dose of about 3.1 x 10^{16} α/g, while 1-length chains reach percolation at 1.4 x 10^{17} α/g.

If we consider the 1-length chain case and estimate the volume fraction of alpha damage using the direct impact model, then percolation sets in when 7.4% of the zircon is occupied by alpha recoil damage zones. This corresponds well with the value of 8.7% obtained by Garboczi et al. (1995) for an ellipsoid of rotation with the same aspect ratio, corroborating the correctness of this calculation and indicating that the slight difference in shape between capsules and ellipsoids of rotation has only a secondary effect. Insofar as a capsule has a higher volume than an ellipsoid of rotation of the same aspect ratio and is thus more likely to be intersected, a slightly lower percolation threshold is the expected result.

Figure 4, showing the evolution of P_{max} with dose for the three alpha recoil track cases, displays the classic pattern of approaching and surpassing a percolation threshold. At low levels of damage few recoil tracks are connected outside of their original chains. However, when a threshold value is reached, the level of interconnectivity rises sharply. Percolation is achieved when only about 5-15% of tracks are connected in a single cluster. By the time the dose is doubled from that point, over 90% of tracks are connected. This growth of P_∞ after the percolation threshold has been surpassed appears to be best characterized with a function of the form:

$$P_\infty = 1 - \left(\frac{p_c}{p}\right)^\beta, \quad (2)$$

where β is a fitted value. The resulting fit is considerably better than the empirical equation form more typical of percolation problems, $P_\infty \propto (p - p_c)^\beta$ (Hunt and Ewing, 2009); the cause of this divergence is not known, but may be due to the continuum nature of this application. Because the increase in amorphous fraction is roughly linear over small intervals of dose, Equation (2) can also be cast in terms of dose:

$$P_\infty = 1 - \left(\frac{D_c}{D}\right)^b, \quad (3)$$

Values of p_c, β, D_c and b for the various cases examined in this paper are provided in Table 5, and the fitted functions are shown in Fig. 4. The poorer fits for the 6-chain and no-chain cases are caused by slight underestimation of P_{max} due to boundary effects, as described previously.

Due to the extremely large aspect ratio of fission tracks, their percolation threshold is reached at approximately 9.8 x 10^{10} FT/g (Table 4). For a zircon grain with only U, this corresponds to an alpha dose of 1.7 x 10^{18} α/g. This equivalent dose will rise with increasing contribution from Th; if Th/U is 0.5, the most typical value for natural zircon (Reiners, 2005), the equivalent alpha dose is 1.9 x 10^{18} α/g. Massive connectivity ($P_\infty > 0.9$) occurs at approximately 6.8 x 10^{18} α/g, assuming Th/U=0.5.

Percolation sets in when 0.0177% of the zircon is occupied by fission damage zones, again corresponding well with the value of 0.0194% obtained from the results of Garboczi et al. (1995) for an ellipsoid of rotation with the same aspect ratio. Figure 5 shows the fission-track equivalent of Fig. 4, illustrating the percolation threshold and the approach to full interconnectivity, along with the corresponding alpha dose assuming a Th/U ratio of 0.5. The same characteristic pattern is seen.

Once alpha recoil damage becomes a fully connected network, all fission tracks will also be connected with that network: if every 25-nm recoil track intersects the infinite cluster, every 16700-nm fission track will as well. We did not test whether fission tracks accelerate alpha recoil damage percolation due to the extreme difference in their length scales, but we do not believe they would have a significant effect. 8-length alpha recoil track chains percolate at a fission-track density of about 10^9 FT/g, which corresponds to an expected occurrence of about 0.1 fission track per 1 μm^3 volume used to test for alpha recoil damage percolation.

Length scales of undamaged volume

The relationship between mean intercept length l_{int} and mean nearest-track distance d_n with dose for alpha recoil and fission tracks is shown in Fig. 6. In all cases, the relationship is near-linear on the logarithmic plot, although there is slight concave-down curvature at high alpha doses; both measures will approach zero when the dose is sufficient for the amorphous fraction to approach 1. In general, d_n is 1-3 orders of magnitude lower than l_{int}, which is not unexpected insofar as the mean intercept length metric only checks for intersections in one direction, and random-point metric in all directions.

Both l_{int} and d_n could be expected to scale with the density of interfaces between damaged and undamaged regions, or in other words the amount of track surface area per crystal volume. Although track intersections lead to a complex reduction in total surface area per track that is highly influenced by track shape and aspect ratio, surface area density can be reasonably approximated as the volume fraction of tracks p times the track surface-to-volume ratio (SV), which is 1.669 nm^{-1} for the capsule approximation of alpha recoil tracks in this study, and 0.741 nm^{-1} for fission tracks.

Figure 7a shows the relationship between the l_{int} and interface density, for both alpha recoil tracks and fission tracks. The slope of the relationship on the log plot is close to -1, indicating that l_{int} is nearly proportional to the inverse of the interface density. Accordingly, we derive the empirical relation

$$l_{int} = \frac{4.2}{p\,SV} - 2.5, \quad (4)$$

where the 4.2 is a dimensionless scaling factor and the 2.5, which has units of nm, may correspond to the alpha recoil track diameter, and thus the amount of traverse length lost per typical intersection. Equation 4 describes our results well to first order (within 6%) for all track types. As p approaches one, l_{int} approaches zero for alpha recoil tracks, indicating that extrapolating to higher p values may be valid for them, but slightly different constants may be required for fission tracks.

As alpha recoil track density rises to 10^{17} α/g, still a relatively low dose for natural zircon, l_{int} for alpha recoil tracks falls to about 40 nm, implying that any atom starting at a random location in undamaged matrix traveling along a straight line (or in a strongly preferred direction, or a concentration gradient vector) will intersect a recoil track within 20 nm on average. If the extrapolation holds to higher doses, then at 10^{18} α/g l_{int} is about 5 nm. For fission tracks, at an equivalent alpha dose of 10^{18} α/g l_{int} is about 70 μm, and falls to about 33 μm at the fission-track percolation threshold. From there it continues to fall, to a predicted value of about 7 μm at a dose of 10^{19} α/g.

A similar result is obtained for d_n. Figure 7b shows d_n as a function of amorphous fraction for both alpha recoil and fission damage; in this case making the two damage types align requires using the square of the surface-to-volume ratio, leading to the function

$$d_n^2 = \frac{3.2}{p\,SV^2} + 1, \quad (5)$$

where 3.2 is again a dimensionless scaling factor, and the 1 has no obvious significance other than helping fit small values. Equation 5 describes both alpha recoil and fission damage cases to within 5% accuracy over the range of scales modeled, but can probably not be extrapolated to p values approaching 1.

Discussion

Comparison with previous work on geometric percolation

The overall similarity of results for non-chained alpha recoil and fission tracks with those of Garboczi et al. (1995) verifies that the calculations in this study are accurate, and that there is not a significant difference between the percolation properties of capsules and ellipsoids of rotation over the range of aspect ratios examined here. The effect of chains on the percolation threshold is interesting, but not surprising. Essentially the chains create "pre-made" networks of damage zones, and thus, even though contact between these networks is less frequent than among fully random tracks, when they occur they cause the total network to expand and ultimately reach percolation much more quickly.

This effect implies that ^{238}Pu-doped zircon (e.g., Weber, 1990) has an important limitation in its ability to serve as a proxy for natural radiation damage over geological time scales, as the decay product of ^{238}Pu is ^{234}U, which has a half-life of 2.455 x 10^5 years. Because

alpha recoil damage will tend to occur as single tracks in this experimental arrangement (i.e. on a laboratory timescale), rather than chains, percolation of alpha recoil damage will require a much higher dose than in natural zircons. Furthermore, insofar as ^{238}Pu generates proportionally ~290 times fewer spontaneous fission tracks per alpha decay than ^{238}U, any effects from percolation of fission-track damage will also be delayed or absent.

Comparison with previous work on percolation in zircon

Accounting for the strong elongation of alpha recoil damage zones, and their occurrence in chains, necessitates a substantial rearrangement of the view of damage percolation in zircon and its possible effects. For a grain containing both U and Th, alpha recoil damage percolation will occur at a dose of about 2.7 x 10^{16} α/g, two orders of magnitude lower than previously considered (Salje et al., 1999; Trachenko et al., 2000). This level of damage is far below what is necessary for zircon metamictization (~10^{19} α/g) and also far below the level typically analyzed when studying radiation damage effects in zircon. This suggests that percolation of alpha recoil damage does not have a large effect on macroscopic swelling and unit cell dimensions, as previously proposed.

However, it is interesting that some behaviors postulated as being caused by alpha recoil damage percolation occur very near to doses at which fission-track damage begins to percolate. Marked changes in the trends of XRD intensity, unit cell parameter *a*, and macroscopic swelling with dose occur at doses between 1 and 2 x 10^{18} α/g in natural zircons (Weber, 1990), which is comparable with the percolation threshold of fission damage. Salje et al. (1999) proposed that percolation marks the point at which macroscopic swelling is matched by the swelling of the unit cell, at an assumed dose of 3.5 x 10^{18} α/g; Zhang et al. (2000) observe a saturation in frequencies

of the Si-O stretching mode at this dose. In both cases, the dose should be corrected by reducing it by a factor of 0.55 to account for damage annealing in the Sri Lankan zircons used (Nasdala et al., 2004), resulting in these transitions occurring at 1.9×10^{18} α/g, which matches the fission-track percolation threshold assuming a Th/U ratio of 0.5.

Figure 8 shows an example of the correlation between material properties and fission-track percolation. The zircon swelling data of Holland and Gottfried (1955) are plotted with corrected dose (Nasdala et al., 2004), and compared with ^{238}Pu-doped zircon measurements by Weber (1990). The natural and artificial data are fairly close to each other until the fission-track percolation transition indicated by the calculations in this study is passed, after which the natural zircons reduce in density much more quickly. Interestingly, the accelerated reduction in density occurs at a rate that is well-matched by the connectivity of fission damage; the model line corresponds to the simplified hypothesis that maximal density reduction will not occur until all fission-track connectivity is maximized. The different density minima of the natural and artificial zircons was attributed by Weber (1990) to the larger initial unit-cell volume and 5.5% porosity and the polycrystalline nature of the ^{238}Pu-doped material, but an additional possibility may be that fission damage is required for maximal density reduction.

Although these are mere correlations at this time, they suggest the hypothesis that fission tracks may exert a larger influence on zircon structure and behavior than previously recognized. One possibility is that fission tracks represent more mechanically important structural discontinuities or weaknesses than alpha recoil tracks, and connectivity of fission tracks facilitates release of pent-up strain from alpha recoil damage as expansion.

A related question that may deserve scrutiny, but is beyond the scope of this study, is whether intersection automatically implies interconnection in the sense of creating a network that facilitates transport, whether of He or other components of interest such as Pb. MD simulations have suggested that an alpha recoil track in zircon may consist of a low-density core mantled by a shell featuring overall increased atomic density (Trachenko et al., 2003). Such a shell could conceivably impede material transfer between some intersecting tracks, perhaps depending on the severity of their impingement. Thus it is possible that alpha recoil tracks could be fast-diffusion pathways (Shuster et al., 2006), but their percolation may not enhance chemical transport. A corollary intuition that may be derived from MD results is that the dense packing and disorder of the damage zone boundary regions would be expected to tend to interrupt transport along favorable directions in the undamaged crystal lattice. However, it should also be borne in mind that the MD simulations only encompass several picoseconds after the decay event, and the damage zone architecture suggested by them may not persist over longer time scales.

Correlation of geometric percolation thresholds with changes in He effective diffusivity

Although alpha recoil track percolation does not appear to correlate with any recognized structural effect, it may be linked to a change in helium diffusivity evolution with dose and by extension closure temperature. Figure 9 shows T_c estimates based on diffusivity measurements by Reiners et al. (2002; 2004), along with the percolation transitions and 90% connectivity levels for alpha recoil and fission tracks. The alpha recoil track percolation threshold and subsequent rise toward full connectivity correlates well with the end of a decline in diffusivity and increase in T_c as dose increases from 10^{16} α/g to just below 10^{17} α/g, and the beginning of a wide range of

doses over which diffusivity appears to change little, if at all, although the data are admittedly sparse.

This leveling may be difficult to reconcile with the idea that radiation damage retards diffusivity primarily by serving as traps, insofar as the number of potential traps rises by more than an order of magnitude without having a significant effect on diffusivity. Furthermore, one might expect the percolation of alpha recoil damage to make the grain more leaky with respect to diffusing helium, but based on available data it appears not to. A possible alternative scenario is that alpha recoil track connectivity may only occasionally result in fast diffusion pathways, and thus offset increasing trap concentration.

It is noteworthy that, although step heating data provide evidence that the entire grain is the effective diffusion domain in at least some zircon specimens (Reiners et al., 2004), the MIL analysis indicates that the spacing between recoil tracks is on the order of hundreds to tens of nanometers at the doses typical of most zircons, and the diffusional length scale suggested by d_n for alpha recoil tracks is an order of magnitude lower still. This observation suggests that, at least with respect to diffusion, the combination of undamaged lattice and recoil damage may be considered as a single material once alpha recoil damage becomes a percolating phase.

On the other hand, correspondence of the steep increase in He effective diffusivity and decreased (U-Th)/He ages at doses greater than 2-4 x 10^{19} α/g in many specimens (Reiners, 2005) with the fission track percolation threshold is consistent with fission tracks exerting a large influence on diffusivity once they are interconnected. A possible mechanism for this drop-off is a radical reduction in the diffusional length scale.

Although alpha recoil tracks evidently do not constitute fast-diffusion pathways for He at the grain scale, fission tracks are an alternative possibility, and the characteristic length scale of diffusion may relate in some way to the spacing between fission tracks. The d_n value for fission tracks approaches 80 nm at a dose of 10^{19} α/g, which corresponds to a characteristic dimension of 160-320 nm by analogy with sheets and spheres, 2.5-3 orders of magnitude smaller than a typical grain and thus leading to an effective diffusivity increase of 5-6 orders of magnitude. Additional enhancement may stem from grain swelling both macroscopically and at the unit cell level.

Tortuosity

The correlation of major changes in He diffusivity evolution with the onset of percolation and progression toward full connectivity provides an additional line of supporting evidence for previous assertions that recoil damage accumulation is probably the principal cause of diffusivity decrease at low damage levels (Shuster et al., 2006; Shuster and Farley, 2009). However, as discussed above, some aspects of the evolution of diffusivity with dose are not intuitive with respect to the mechanism of trapping. An alternative mechanism may be expressed as an increase in tortuosity, or the length and difficulty of interatomic pathways that He atoms must traverse in order to exit from the grain.

Modeling studies and theoretical considerations (Bengston et al., 2012; Farley, 2007; Reich et al., 2007; Saadoune and De Leeuw, 2009) strongly suggest He will diffuse much more quickly along the zircon *c*-axis than in other directions in an ideal, undamaged lattice. Reich et al. (2007) calculate from MD modeling that the activation energy required for tracer diffusion along the *c*-axis direction is 13.4 kJ mol^{-1} along [001], as compared with 44.8, 101.7, and 421.3

kJ mol^{-1} along [100], [101], and [110], corresponding to a difference in diffusivity of many orders of magnitude. This extreme anisotropy is generally corroborated by density functional theory analysis (Bengston et al., 2012; Saadoune et al., 2009). However, these results are only weakly matched by experimental results by Cherniak et al. (2009), who find only a two orders-of-magnitude difference in diffusivity with direction. Bengston et al. (2012) hypothesized that this mismatch may be due to radiation damage at the nm level, the scale of individual damage features, and that this damage may serve to reduce bulk anisotropy, an idea corroborated by the calculations of effects from specific defects by Saadoune et al. (2009).

While dispersed individual damage features such as isolated cascades and point defects may indeed contribute to such an effect, the results of this study suggest a different length scale on which the aggregate effect of radiation damage might be productively considered. For example, even at exceedingly low damage levels of 10^{15} α/g (corresponding to a 32 ppm eU grain accumulating damage over 10 Ma), calculations here indicate that the mean distance between recoil-damaged regions along a straight line is on the order of 5 μm, and thus all fast crystallographic pathways in a grain will be interrupted by damage. If the amorphous structure of damage trails impedes or prevent passage of He atoms, the most energetically favorable direction for a diffusing atom to travel after encountering a blockage may well be back the way it came. Moreover, even after the atom makes energetically more difficult jumps to neighboring *c*-axis-parallel channels, these are likely to also be blocked by recoil damage. It is thus apparent that damage will tend to decrease the effects of crystallographic anisotropy in transport favorability, and decrease overall diffusivity both by lengthening travel paths and requiring jumps with less favorable energetics.

It is also possible that straightforward interpretation of diffusivity measurements undertaken by microanalytical techniques near grain surfaces may be complicated by not detecting or accounting for the effect of interruptions on larger length scales. For example, Cherniak et al. (2009) implanted ^{3}He into zircon at a depth of 380 nm with FWHM spread of 83 nm and measured its diffusional dispersion. Of the two zircons they analyzed, only the Mud Tank had sufficient information to estimate alpha dose (~1.2 x 10^{16} α/g), and its estimated l_{int} for alpha recoil damage is on the order of 350 nm. The similarity of length scale suggests that their measurements may contain some effect from recoil damage tracks, but they probably principally reflect undamaged material (crudely, about half of particle paths normal to the surface may be interrupted, perhaps affecting transport by a factor of up to 2.). As a result, it is unclear whether the He retentivity of an entire grain will be fully characterized by measurements at this scale.

A mechanism of tortuosity as opposed to trapping may also explain the observation by Shuster and Farley (2009) for relatively low-damage apatite that natural alpha recoil damage and damage induced by neutron irradiation appear to have nearly equivalent effects on diffusivity as a function of their kerma, or total kinetic energy deposited as ionization. Although the character of each damage type is expected to be different, the number of atomic displacements, and thus possible interruptions to favorable diffusion pathways, will be similar. If traps are conceived of as discrete zones, however, then one might expect the more dispersed effects of neutron irradiation to have a different effect.

Because tortuosity is difficult to quantify from first principles in many situations (Clennell, 1997), tortuosity effects on diffusivity are often applied as an empirical correction and expressed as a direct scaling factor with the same general form as the partitioning factor used for the trapping model equation (Crank, 1975; Farley, 2000; Trull et al., 1991). Thus, even though

the mechanism for diffusivity reduction may be different than previously postulated, the equation summarizing how radiation damage affects diffusivity may be similar, and existing formulations based on the idea of trapping (Flowers et al., 2009; Gautheron et al., 2009; Shuster et al., 2006) may still be appropriate, at least at low damage levels.

However, it bears notice that the diffusivity data for apatite summarized by Flowers et al. (2009, Fig. 1) shows evidence of a possible plateau in closure temperature, and by extension effective diffusivity, at effective fission-track densities exceeding ~2.5 x 10^6 tracks/cm^2, which roughly corresponds to a dose of 1.8 x 10^{16} α/g, very close to the percolation transition for alpha recoil damage in zircon (~3 x 10^{16} α/g). Insofar as apatite features longer stopping distances than zircon due to its lower density, its percolation transition will be at a somewhat lower dose. However, calculating the percolation threshold for apatite (or any other mineral of interest) will require modeling incorporating specific knowledge of recoil track properties (length, diameter, volume) in that mineral. If we assume that the only difference between apatite and zircon is in mean recoil nucleus stopping distance (31.5 μm vs. 25 μm) then extrapolating the results of Garboczi et al. (1995) indicates that the percolation threshold occurs at a damage volume fraction ~15% below that for zircon. It is thus possible that percolation of alpha recoil damage correlates with a transition in apatite diffusivity behavior as well, though apatites with such high levels of damage will only be infrequently encountered, in part because recoil damage annealing occurs at lower temperatures (Shuster and Farley, 2009).

Conclusions

Accounting for the elongation and clustering of radiation damage zones necessitates a substantial re-evaluation of the possible effects of damage percolation and connectivity on zircon

material properties. Alpha recoil track percolation does not correlate with any previously measured transition in macroscopic or unit cell properties, but may be linked to establishing a minimum in helium diffusivity, whereas fission track percolation correlates well with increases in grain swelling rate and diffusivity. The influence of fission damage on zircon structural and chemical integrity has previously been considered negligible due to its low abundance, but it may constitute an important difference between natural and man-made materials being considered for sequestration of radioactive elements.

Acknowledgements

We wish to thank the Geology Foundation of the Jackson School of Geosciences for support of this work. Communications with R. Devanathan were very helpful, and thorough reviews by D. Shuster and D. Cherniak improved the manuscript.

References

Bengston, A., Ewing, R.C., and Becker, U. (2012) He diffusion and closure temperatures in apatite and zircon: A density functional theory investigation. Geochimica et Cosmochimica Acta, 86, 228-238.

Carlson, W.D. (1990) Mechanisms and kinetics of apatite fission-track annealing. American Mineralogist, 75, 1120-1139.

Cherniak, D.J., Watson, E.B., and Thomas, J.B. (2009) Diffusion of helium in zircon and apatite. Chemical Geology, 268, 155-166.

Clennell, M.B. (1997) Tortuosity: a guide through the maze. Geological Society, London, Special Publications, 122, 299-344.

Crank, J. (1975) The Mathematics of Diffusion. Clarendon, Oxford.

Devanathan, R., Corrales, L.R., Weber, W.J., Chartier, A., and Meis, C. (2006) Molecular cynamics simulation of energetic uranium recoil damage in zircon. Molecular Simulation, 32(12-13), 1069-1077.

Ewing, R.C., Meldrum, A., Wang, L., Weber, W.J., and Corrales, L.R. (2003) Radiation effects in zircon. Reviews in Mineralogy and Geochemistry, 53, 387-425.

Farley, K.A. (2000) Helium diffusion from apatite: General behavior as illustrated by Durango fluorapatite. Journal of Geophysical Research, 105(B2), 2903-2914.

Farley, K.A. (2007) He diffusion systematics in minerals: Evidence from synthetic monazite and zircon structure phosphates. Geochimica et Cosmochimica Acta, 71, 4015-4024.

Flowers, R.M., Ketcham, R.A., Shuster, D.L., and Farley, K.A. (2009) Apatite (U-Th)/He thermochronometry using a radiation damage accumulation and annealing model. Geochimica et Cosmochimica Acta, 73(8), 2347-2365.

Garboczi, E.J., Snyder, K.A., Douglas, J.F., and Thorpe, M.F. (1995) Geometric percolation threshold of overlapping ellipsoids. Physical Review E, 52(1), 819-828.

Gautheron, C., Tassan-Got, L., Barbarand, J., and Pagel, M. (2009) Effect of alpha-damage annealing on apatite (U-Th)/He thermochronology. Chemical Geology, 266, 157-170.

Gibbons, J.F. (1972) Ion implantation in semiconductors - Part II: Damage production and annealing. Proceedings of the IEEE, 60(9), 1062-1096.

Gögen, K., and Wagner, G.A. (2000) Alpha-recoil track dating of Quaternary volcanics. Chemical Geology, 166, 127-137.

Holland, H.D. (1954) Radiation damage and energy storage. In H. Faul, Ed. Nuclear Geology, p. 175-179. John Wiley & Sons, New York.

Holland, H.D., and Gottfried, D. (1955) The effect of nuclear radiation on the structure of zircon. Acta Crystallographica, 8, 291-200.

Hunt, A.G., and Ewing, R.P. (2009) Percolation Theory for Flow in Porous Media. Springer-Verlag, Berlin.

Hurley, P.M. (1954) The helium age method and the distribution and migration of helium in rocks. In H. Faul, Ed. Nuclear Geology, p. 301-328. John Wiley & Sons, New York.

Hurley, P.M., Larsen, E.S.J., and Gottfried, D. (1956) Comparison of radiogenic helium and lead in zircon. Geochimica et Cosmochimica Acta, 9(1-2), 98-102.

Jonckheere, R. (2003) On the densities of etchable fission tracks in a mineral and co-irradiated external detector with reference to fission-track dating of minerals. Chemical Geology, 200, 41-58.

Jonckheere, R., and Gögen, K. (2001) A Monte-Carlo calcultion of the size distribution of latent alpha-recoil tracks. Nuclear Instruments and Methods in Physics Research B, 183, 347-357.

Lang, M., Lian, J., Zhang, F., Hendricks, B.W.H., Trautmann, C., Neumann, R., and Ewing, R.C. (2008) Fission tracks simulated by swift heavy ions at crustal pressures and temperatures. Earth and Planetary Science Letters, 274, 355-358.

Li, W., Lang, M., Gleadow, A.J.W., Zdorvets, M.V., and Ewing, R.C. (2012) Thermal annealing of unetched fission tracks in apatite. Earth and Planetary Science Letters, 321-322, 121-127.

Nasdala, L., Reiners, P.W., Garver, J.I., Kennedy, A.K., Stern, R.A., Balan, E., and Wirth, R. (2004) Incomplete retention of radiation damage in zircon from Sri Lanka. American Mineralogist, 89, 219-231.

Nasdala, L., Wenzel, M., Vavra, G., Irmer, G., Wenzel, T., and Kober, B. (2001) Metamictization of natural zircon: accumulation versus thermal annealing of radioactivity-induced damage. Contributions to Mineralogy and Petrology, 141, 125-144.

Palenik, C.S., Nasdala, L., and Ewing, R.C. (2003) Radiation damage in zircon. American Mineralogist, 88, 770-781.

Reich, M., Ewing, R.C., Ehlers, T.A., and Becker, U. (2007) Low-temperature anisotropic diffusion of helium in zircon: Implications for zircon (U-Th)/He thermochronometry. Geochimica et Cosmochimica Acta, 71(12), 3119-3130.

Reiners, P.W. (2005) Zircon (U-Th)/He thermochronometry. Reviews in Mineralogy and Geochemistry, 58, 151-179.

Reiners, P.W., Farley, K.A., and Hickes, H.J. (2002) He diffusion and (U-Th)/He thermochronometry of zircon: initial results from Fish Canyon Tuff and Gold Butte. Tectonophysics, 349, 297-308.

Reiners, P.W., Spell, T.L., Nicolescu, S., and Zanetti, K.A. (2004) Zircon (U-Th)/He thermochronometry: He diffusion and comparisons with $^{40}Ar/^{39}Ar$ dating. Geochimica et Cosmochimica Acta, 68(8), 1857-1887.

Ríos, S., Salje, E.K.H., Zhang, M., and Ewing, R.C. (2000) Amorphization in zircon: evidence for direct impact damage. Journal of Physics: Condensed Matter, 12, 2401-2412.

Saadoune, I., and De Leeuw, N.H. (2009) A computer simulation study of the accommodation and diffusion of He in uranium- and plutonium-doped zircon ($ZrSiO_4$). Geochimica et Cosmochimica Acta, 73, 3880-3893.

Saadoune, I., Purton, J.A., and de Leeuw, N.H. (2009) He incorporation and diffusion pathways in pure and defective zircon $ZrSiO_4$: A density functional theory study. Chemical Geology, 258, 182-196.

Salje, E.K.H., Chrosch, J., and Ewing, R.C. (1999) Is "metamictization" of zircon a phase transition? American Mineralogist, 84, 1107-1116.

Shuster, D.L., and Farley, K.A. (2009) The influence of artificial radiation damage and thermal annealing on helium diffusion kinetics in apatite. Geochimica et Cosmochimica Acta, 73, 183-196.

Shuster, D.L., Flowers, R.M., and Farley, K.A. (2006) The influence of natural radiation damage on helium diffusion kinetics in apatite. Earth and Planetary Science Letters, 249, 148-161.

Trachenko, K., Dove, M.T., and Salje, E.K.H. (2000) Modeling the percolation-type transition in radiation damage. Journal of Applied Physics, 87(11), 7702-7707.

Trachenko, K., Dove, M.T., and Salje, E.K.H. (2002) Structural changes in zircon under a-decay irradiation. Physical Review B, 65, 180102-(1-3).

Trachenko, K., Dove, M.T., and Salje, E.K.H. (2003) Large swelling and percolation in irradiated zircon. Journal of Physics: Condensed Matter, 15, L1-L7.

Trull, T.W., Kurz, M.D., and Jenkins, W.J. (1991) Diffusion of cosmogenic ^3He in olivine and quartz: implications for surface exposure dating. Earth and Planetary Science Letters, 103, 241-256.

Weber, W.J. (1990) Radiation-induced defects and amorphization in zircon. Journal of Materials Research, 5(11), 2687-2697.

Weber, W.J., Ewing, R.C., and Wang, L.-M. (1994) The radiation-induced crystalline-to-amorphous transition in zircon. Journal of Materials Research, 9(3), 688-698.

Zhang, M., Salje, E.K.H., Farnan, I., Graeme-Barber, A., Daniel, P., Ewing, R.C., Clark, A.M., and Leroux, H. (2000) Metamictization of zircon: Raman spectroscopic study. Journal of Physics: Condensed Matter, 12, 1915-1925.

Ziegler, J.F., Biersack, J.P., and Ziegler, M.D. (2008) SRIM The Stopping and Range of Ions in Matter. 390 p. SRIM Co., Chester, Maryland.

Figure Captions

Figure 1. Simple example of percolation as expressed on a 2D grid, illustrating meaning of p, p_c, P_{max}, and P_∞ as defined in the text.

Figure 2. (a) Damage tracks are represented as capsules, which are defined by the set of points at a constant radial distance from a line segment. (b) Idealized depiction of alpha recoil damage zone caused by complete sequence of decays in the ^{232}Th decay chain. It is assumed that beta decays do not cause sufficient displacement to disrupt the damage chain.

Figure 3. Schematic illustration of metrics used to characterize undamaged regions. The mean intercept length (l_{int}) is calculated by projecting traverses through the model space, and counting intersections with damage tracks; l_{int} is equal to the total length of all traverses divided by the number of all intercepts (i.e. 2L/(7+2) in this example). The mean nearest-neighbor distance d_n is calculated by placing a series of N random points into undamaged areas, determining the distance $d_{n,1..N}$ from each one to the nearest damage zone, and taking their mean. Although this illustration is 2D, calculations are 3D.

Figure 4. Proportion of tracks in the largest connected cluster (P_{max}) as a function of dose for alpha recoil tracks in chains of 8, 6, and 1. Lines are fits according to Equation 2 and values in Table 5. Percolation occurs soon after the sudden rise in each curve, at a P_{max} value of 0.5-0.15.

Figure 5. Proportion of fission tracks in largest connected cluster as a function of fission dose and alpha dose. Line is fit according to Equation 2 and values in Table 5.

Figure 6. Relationship of mean intercept length l_{int} and mean distance from a random point in undamaged crystal to the nearest track d_n to dose for (a) alpha recoil and (b) fission tracks.

Figure 7. Relationship of (a) l_{int} to interface density, and (b) d_n and the squared interface density,

Figure 8. Comparison of macroscopic swelling of ^{238}Pu-doped zircon (Weber, 1990) and natural zircon (Holland and Gottfried, 1955, with doses corrected according to Nasdala et al., 2004), and its possible relationship with the percolation and rise to full connectivity of fission damage. The equation scales the density transition between crystalline and metamict zircon (ρ_c and ρ_m) with proportion of fission-tracks connected to the infinite cluster (P_∞).

Figure 9. Relationship of percolation and connectivity of alpha recoil and fission damage to He diffusivity determinations by Reiners et al. (2002, 2004). As dose approaches 10^{19} α/g grains are expected to become less retentive, based on observations of progressively lower ages in suites of ages in grains with varying U and Th content (e.g. Reiners 2005).

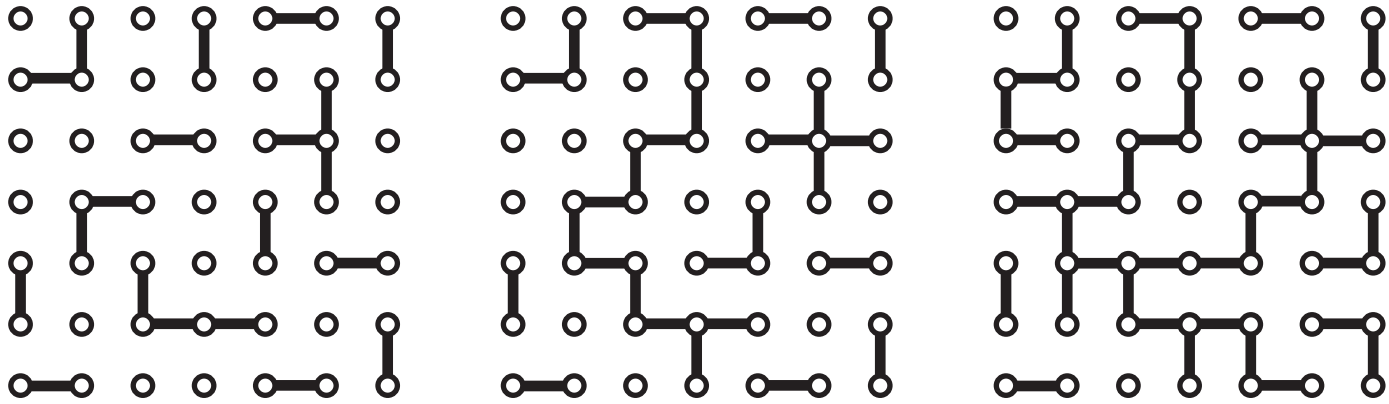

$p = 20/84 = 0.24$
$P_{max} = 3/20 = 0.15$

$p = 26/84 = 0.31 = p_c$
$P_{max} = P_\infty = 12/28 = 0.43$

$p = 38/84 = 0.45 > p_c$
$P_{max} = P_\infty = 24/38 = 0.63$

Figure 1

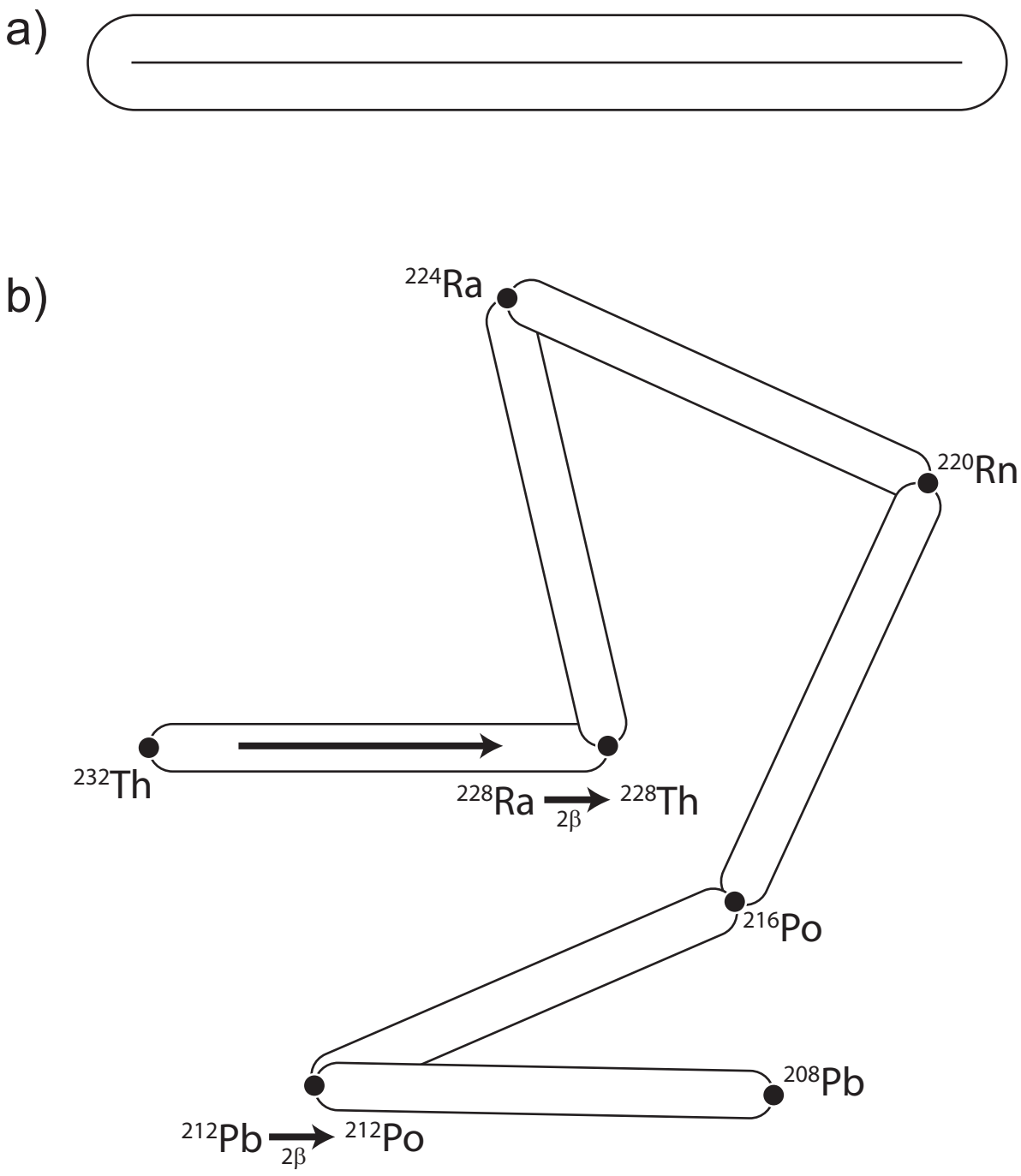
a)
b)
224Ra
220Rn
232Th
228Ra
2β
228Th
216Po
208Pb
212Pb
2β
212Po

Figure 2

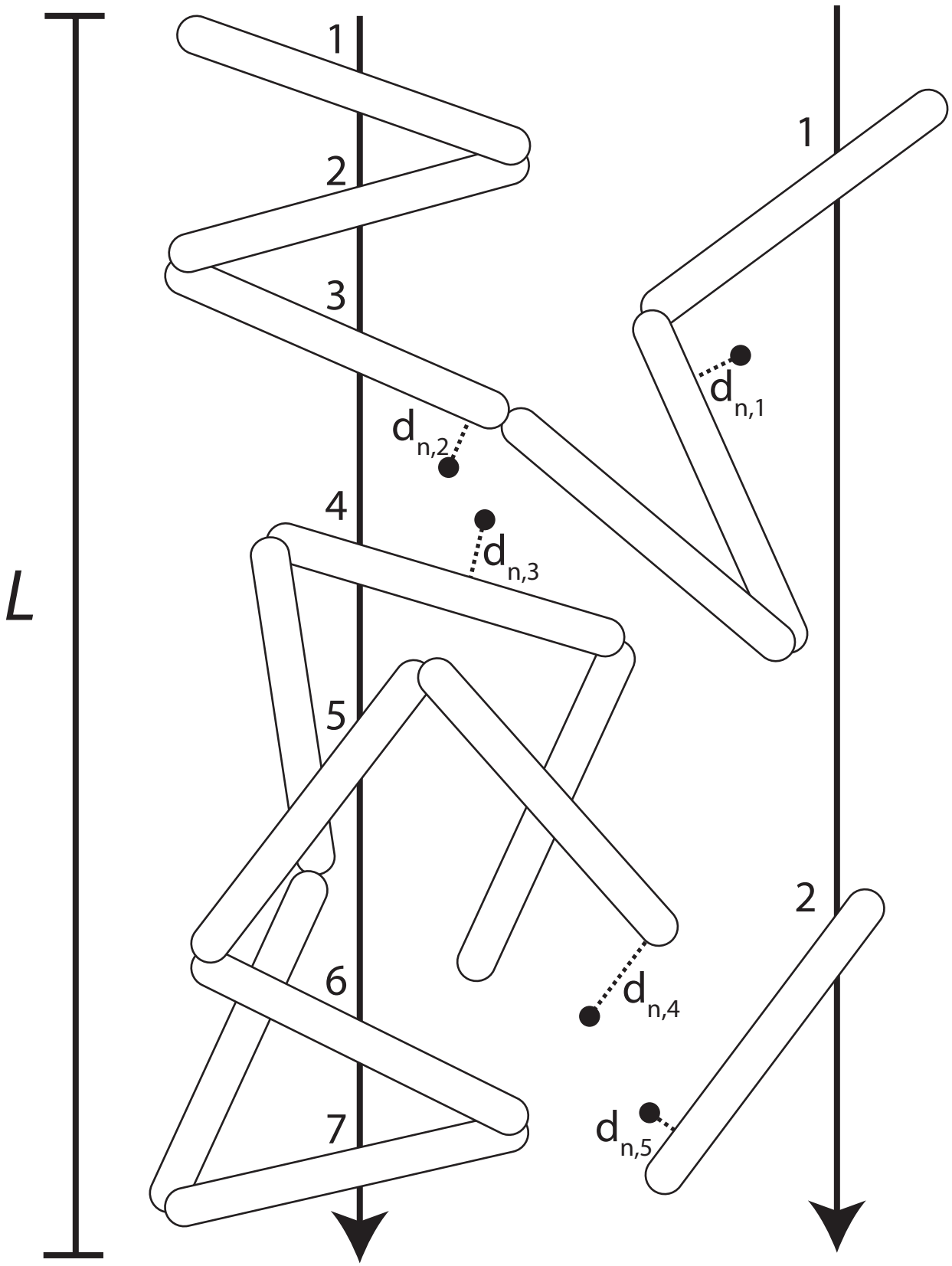

Figure 3

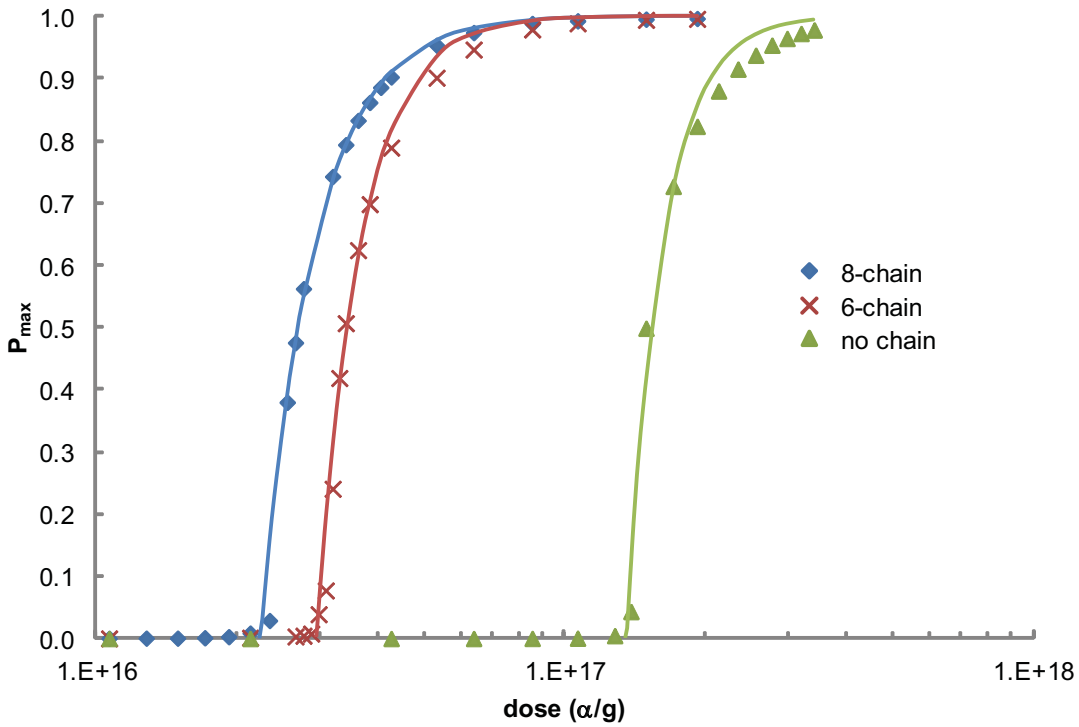
1.0
0.9
0.8
0.7
0.6
0.5
0.4
0.3
0.2
0.1
0.0
P max
1.E+16
1.E+17
1.E+18
dose (α/g)
8-chain
6-chain
no chain

Figure 4

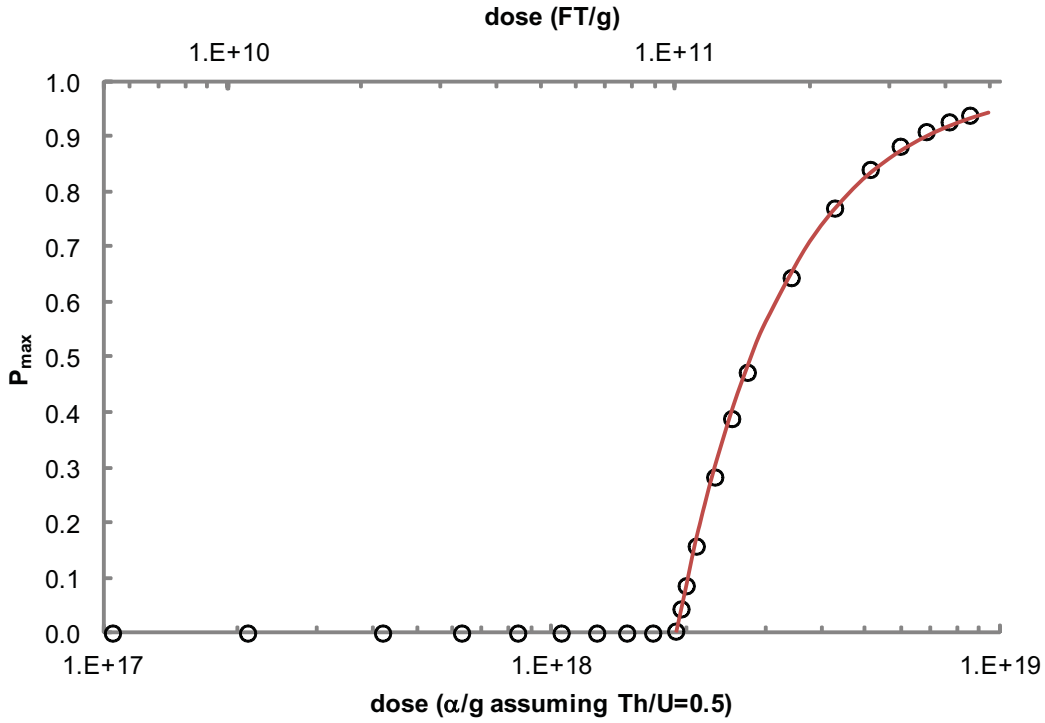
dose (FT/g)
1.E+10
1.E+11
1.0
0.9
0.8
0.7
0.6
0.5
0.4
0.3
0.2
0.1
0.0
P_{max}
1.E+17
1.E+18
1.E+19
dose (α/g assuming Th/U=0.5)

Figure 5

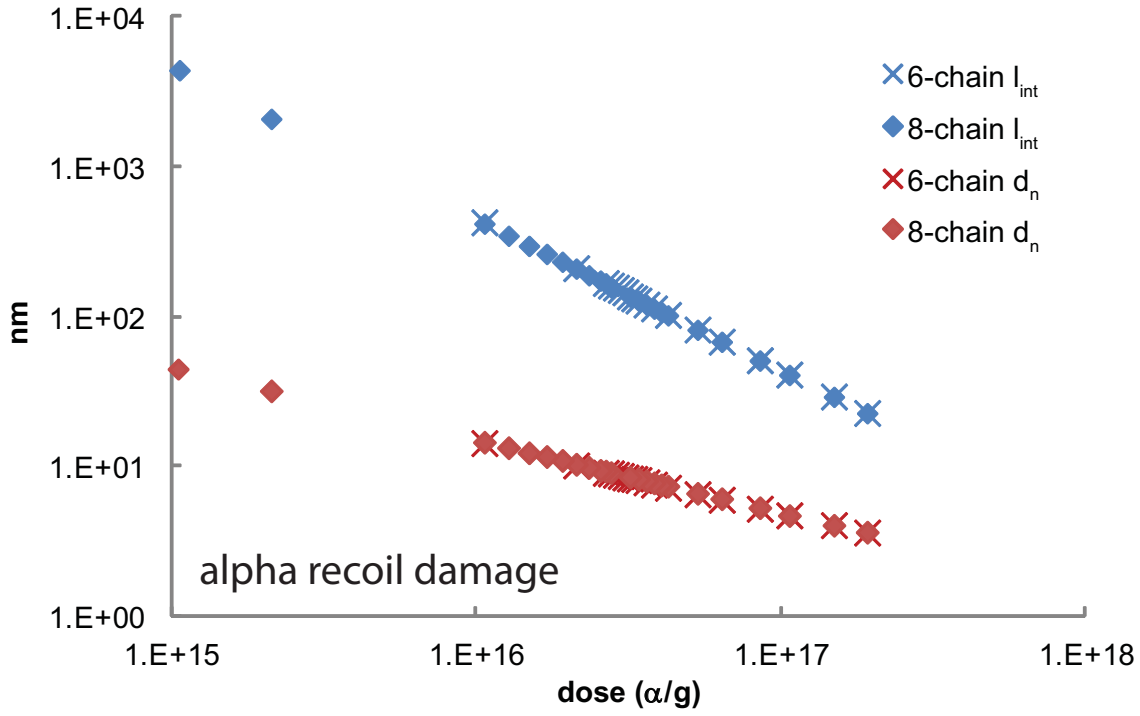
1.E+04
1.E+03
1.E+02
1.E+01
1.E+00
nm
6-chain l_{int}
8-chain l_{int}
6-chain d_n
8-chain d_n
alpha recoil damage
1.E+15
1.E+16
1.E+17
1.E+18
dose (α/g)

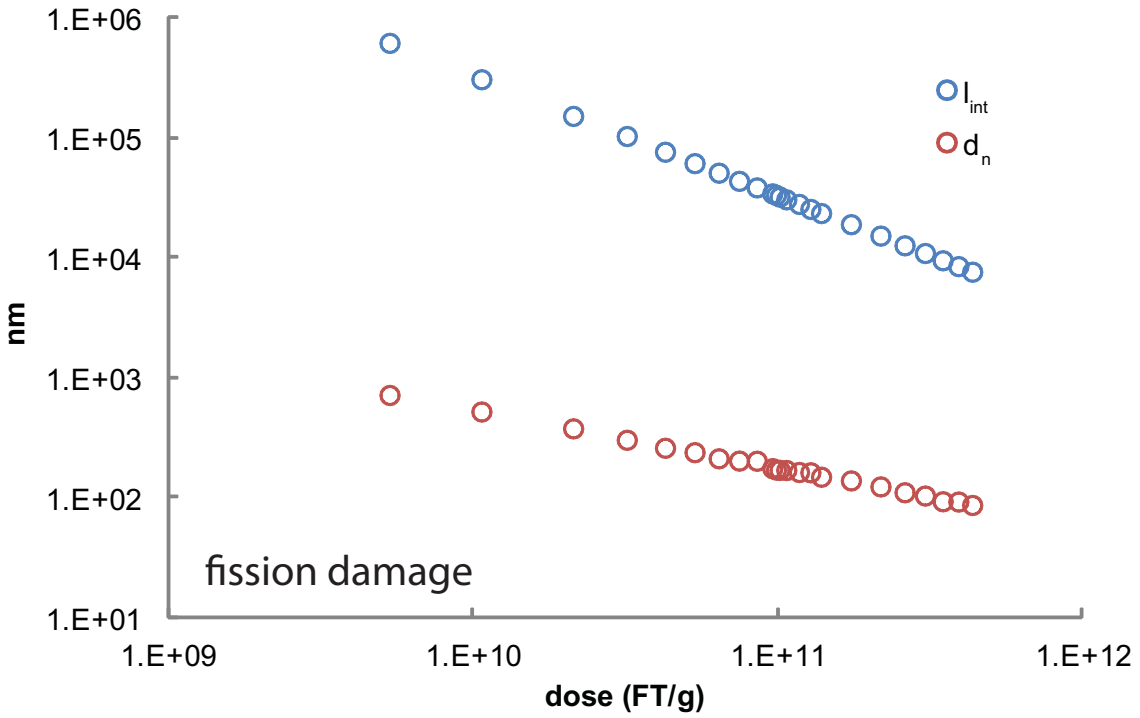
1.E+06
1.E+05
1.E+04
1.E+03
1.E+02
1.E+01
nm
l_{int}
d_n
fission damage
1.E+09
1.E+10
1.E+11
1.E+12
dose (FT/g)

Figure 6

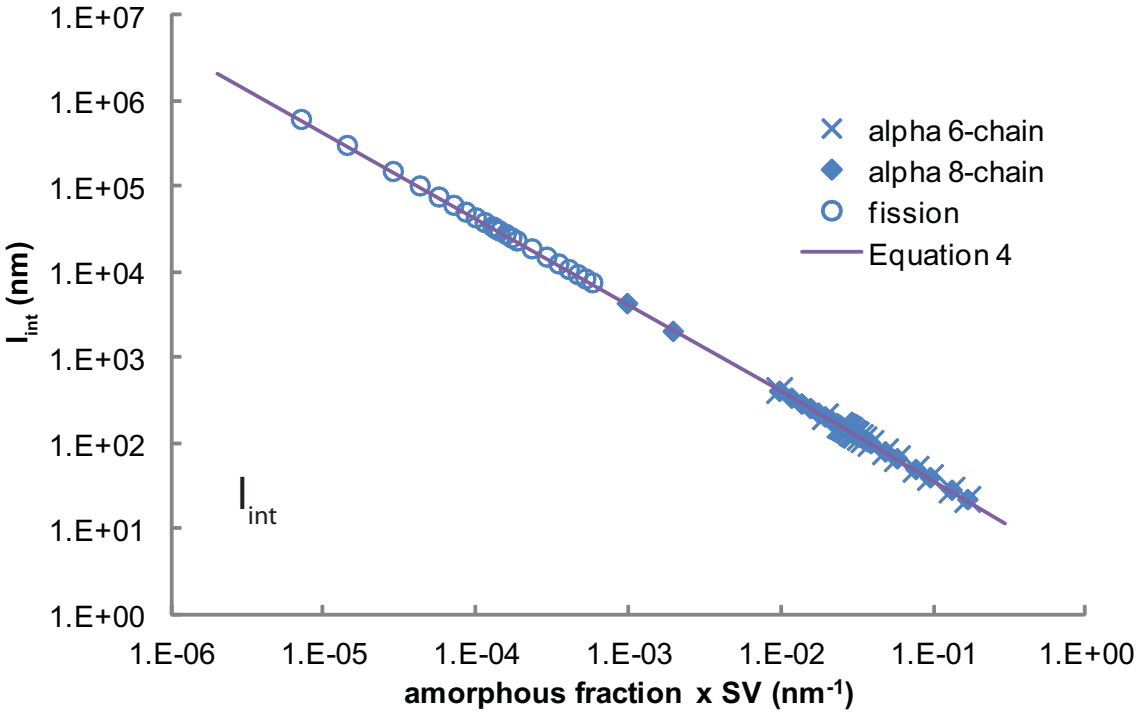
1.E+07
1.E+06
1.E+05
1.E+04
1.E+03
1.E+02
1.E+01
1.E+00
I_{int} (nm)
alpha 6-chain
alpha 8-chain
fission
Equation 4
I_{int}
1.E-06
1.E-05
1.E-04
1.E-03
1.E-02
1.E-01
1.E+00
amorphous fraction x SV (nm^{-1})

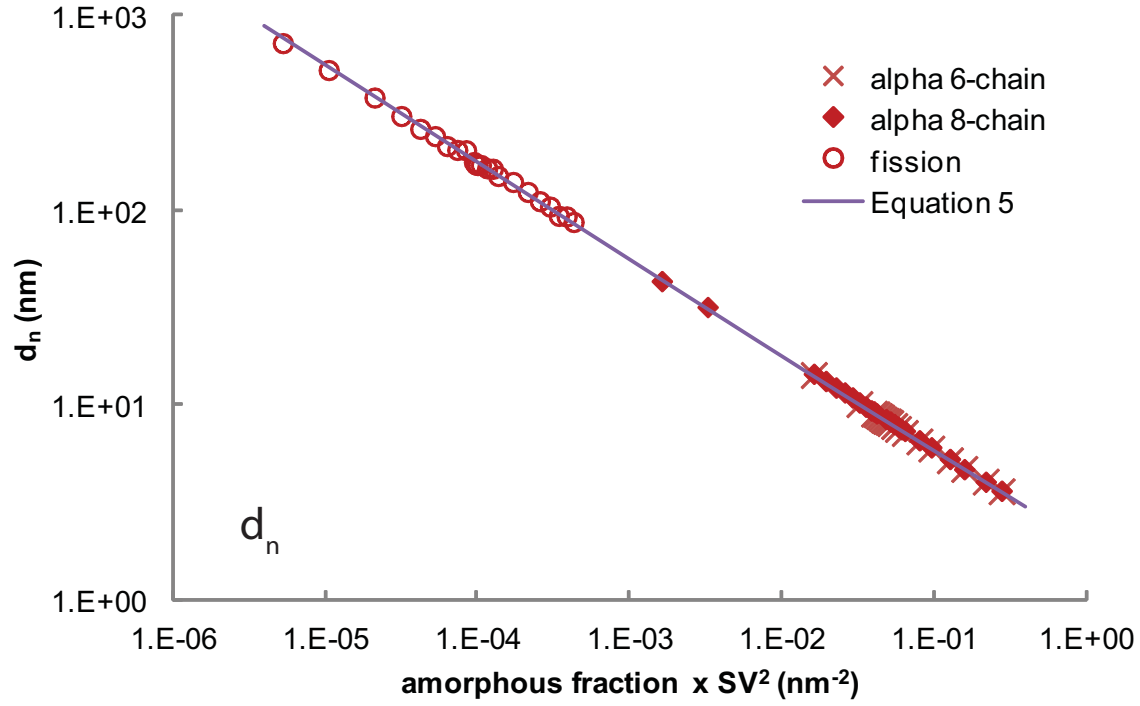
1.E+03
1.E+02
1.E+01
1.E+00
d_n (nm)
alpha 6-chain
alpha 8-chain
fission
Equation 5
d_n
1.E-06
1.E-05
1.E-04
1.E-03
1.E-02
1.E-01
1.E+00
amorphous fraction x SV^2 (nm^{-2})

Figure 7

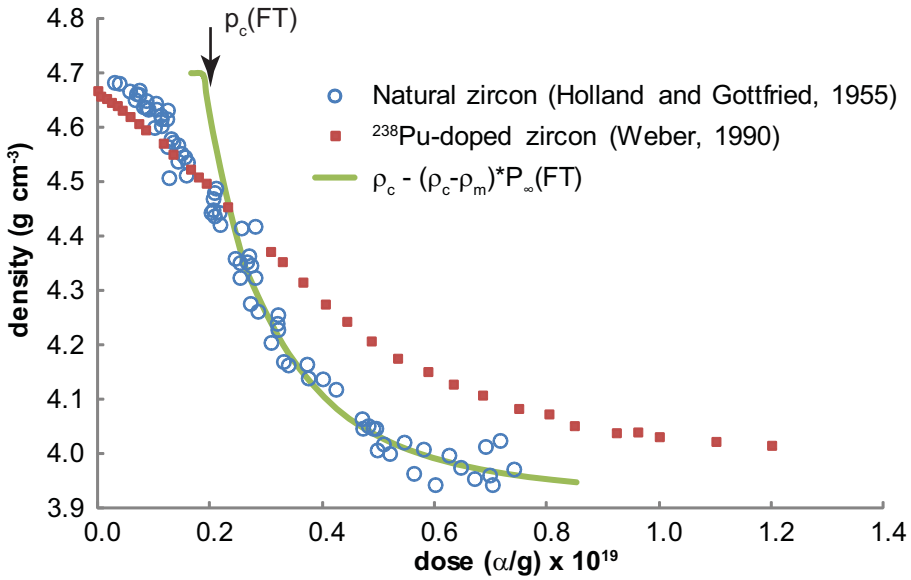
4.8
4.7
4.6
4.5
4.4
4.3
4.2
4.1
4.0
3.9
density (g cm-3)
0.0
0.2
0.4
0.6
0.8
1.0
1.2
1.4
dose (α/g) x 10^19
pc(FT)
Natural zircon (Holland and Gottfried, 1955)
238Pu-doped zircon (Weber, 1990)
ρc - (ρc-ρm)*P∞(FT)

Figure 8

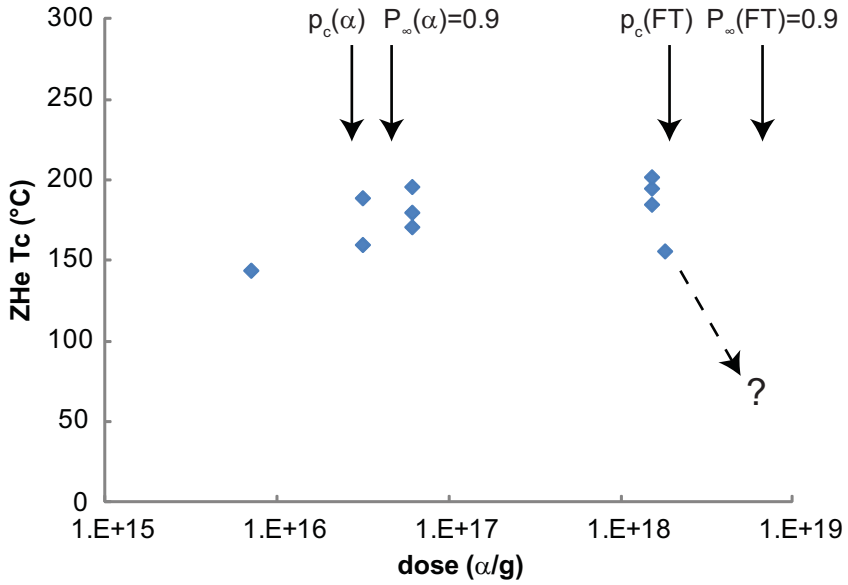
300
250
200
150
100
50
0
ZHe Tc (°C)
1.E+15
1.E+16
1.E+17
1.E+18
1.E+19
dose (α/g)
p_c(α)
P_∞(α)=0.9
p_c(FT)
P_∞(FT)=0.9
?

Figure 9

Table 1. Modeling results for alpha recoil tracks generated in 8-length chains

Dose (α/g x 10^{17})	p	Int./α	Sides	P_{max}	l_{int} (nm)	d_n (nm)
1.9149	0.0996	0.1285	6	0.997	22.8	3.66
1.4894	0.0784	0.1281	6	0.996	29.3	4.07
1.0638	0.0566	0.1273	6	0.993	40.9	4.72
0.8511	0.0456	0.1264	6	0.989	51.1	5.33
0.6383	0.0344	0.1245	6	0.975	68.2	6.11
0.5319	0.0287	0.1222	6	0.954	82.0	6.65
0.4255	0.0230	0.1173	6	0.903	102.2	7.42
0.4043	0.0219	0.1160	6	0.887	107.8	7.56
0.3830	0.0208	0.1142	6	0.862	113.3	7.81
0.3617	0.0196	0.1121	6	0.833	120.4	8.05
0.3404	0.0185	0.1096	6	0.794	128.1	8.30
0.3191	0.0173	0.1067	6	0.743	136.4	8.54
0.2766	0.0150	0.0988	6	0.563	157.3	9.14
0.2660	0.0145	0.0970	6	0.476	167.4	9.35
0.2553	0.0139	0.0945	6	0.380	174.4	9.45
0.2340	0.0127	0.0884	1	0.029	189.2	9.89
0.2128	0.0116	0.0820	1	0.009	209.7	10.39
0.1915	0.0104	0.0759	0	0.003	233.0	11.02
0.1702	0.0093	0.0680	0	0.001	262.7	11.70
0.1489	0.0081	0.0605	1	0.001	297.3	12.40
0.1277	0.0070	0.0530	0	0.001	347.4	13.39
0.1064	0.0058	0.0444	1	0.001	418.3	14.58
0.0213	0.0012	0.0088	0	0.001	2092.5	32.09
0.0106	0.0006	0.0045	0	0.001	4416.0	43.57

Dose may be converted to nmol He/g, assuming full He retention, by multiplying by $166/10^{17}$.
Int/α = track intersections per alpha particle, not including intersections along chains.
Sides = number of sides of cubic volume intersected by largest cluster (6 indicates full percolation).

Table 2. Modeling results for alpha recoil tracks generated in 6-length chains

Dose (α/g x 10^{17})	p	Int./α	Sides	P_{max}	l_{int} (nm)	d_n (nm)
1.9149	0.0996	0.1700	6	0.997	22.8	3.64
1.4894	0.0784	0.1694	6	0.995	29.4	4.08
1.0638	0.0566	0.1680	6	0.990	41.2	4.74
0.8511	0.0456	0.1662	6	0.980	51.3	5.25
0.6383	0.0344	0.1614	6	0.947	68.3	6.03
0.5319	0.0287	0.1560	6	0.902	82.3	6.55
0.4255	0.0230	0.1453	6	0.790	103.0	7.24
0.3830	0.0208	0.1388	6	0.699	113.7	7.60
0.3617	0.0196	0.1348	6	0.625	120.8	7.87
0.3404	0.0185	0.1295	6	0.507	128.3	8.15
0.3298	0.0179	0.1272	6	0.419	132.7	8.29
0.3191	0.0173	0.1241	6	0.241	136.8	8.35
0.3085	0.0168	0.1218	5	0.077	145.8	8.48
0.2979	0.0162	0.1186	2	0.039	151.0	8.68
0.2872	0.0156	0.1148	0	0.008	156.7	8.84
0.2766	0.0150	0.1120	1	0.005	161.7	9.03
0.2660	0.0145	0.1079	0	0.003	168.1	9.11
0.2128	0.0116	0.0900	0	0.001	211.1	10.20
0.1064	0.0058	0.0474	0	0.000	427.1	14.38

Dose may be converted to nmol He/g, assuming full He retention, by multiplying by $166/10^{17}$.
Int/α = track intersections per alpha particle, not including intersections along chains.
Sides = number of sides of cubic volume intersected by largest cluster (6 indicates full percolation).

Table 3. Modeling results for alpha recoil tracks generated without chains

Dose (α/g x 10^{17})	p	Int./α	Sides	P_{max}	l_{int} (nm)	d_n (nm)
3.4043	0.1702	0.9820	6	0.979	13.6	2.75
3.1915	0.1605	0.9775	6	0.973	14.4	2.82
2.9787	0.1506	0.9712	6	0.965	15.5	2.92
2.7660	0.1406	0.9634	6	0.954	16.7	3.00
2.5532	0.1306	0.9520	6	0.938	18.1	3.06
2.3404	0.1204	0.9376	6	0.916	19.7	3.15
2.1277	0.1101	0.9166	6	0.881	21.7	3.28
1.9149	0.0996	0.8874	6	0.824	24.2	3.43
1.7021	0.0891	0.8468	6	0.727	27.1	3.59
1.4894	0.0784	0.7885	6	0.499	31.0	3.74
1.3830	0.0730	0.7511	2	0.043	33.4	3.89
1.2766	0.0676	0.7093	1	0.005	36.1	4.01
1.0638	0.0566	0.6132	0	0.001	43.5	4.31
0.8511	0.0456	0.5067	0	0.000	54.4	4.74
0.6383	0.0344	0.3930	0	0.000	72.6	5.32
0.4255	0.0230	0.2684	0	0.000	108.4	6.33
0.2128	0.0116	0.1374	0	0.000	230.9	8.47
0.1064	0.0058	0.0712	0	0.000	466.6	11.27
0.0213	0.0012	0.0160	0	0.000	2328.8	21.40
0.0106	0.0006	0.0094	0	0.001	5399.6	27.70

Dose may be converted to nmol He/g, assuming full He retention, by multiplying by $166/10^{17}$.
Int/α = track intersections per alpha particle, not including intersections along chains.
Sides = number of sides of cubic volume intersected by largest cluster (6 indicates full percolation).

Table 4. Modeling results for fission tracks

FT Dose (FT/g x 10^{11})	α Dose (U only) (α/g x 10^{18})	α Dose (Th/U = 0.5) (α/g x 10^{18})	p	Int./FT	Sides	P_{max}	l_{int} (μm)	d_n (nm)
4.3307	7.622	8.529	0.00078	0.9442	6	0.940	7.7	87.7
3.8976	6.860	7.676	0.00070	0.9337	6	0.928	8.6	93.7
3.4645	6.098	6.823	0.00062	0.9185	6	0.910	9.6	94.4
3.0315	5.335	5.970	0.00054	0.8965	6	0.883	11.1	105.2
2.5984	4.573	5.117	0.00047	0.8633	6	0.841	12.8	112.1
2.1653	3.811	4.265	0.00039	0.8119	6	0.771	15.5	125.2
1.7323	3.049	3.412	0.00031	0.7304	6	0.645	19.3	140.7
1.3830	2.434	2.724	0.00025	0.6403	6	0.473	23.9	151.0
1.2766	2.247	2.514	0.00023	0.6009	6	0.389	25.8	164.6
1.1702	2.060	2.305	0.00021	0.5569	6	0.283	28.4	165.3
1.0638	1.872	2.095	0.00019	0.5103	6	0.158	31.0	171.9
1.0106	1.779	1.990	0.00018	0.4860	6	0.086	32.7	172.1
0.9840	1.732	1.938	0.00018	0.4723	6	0.044	33.8	173.1
0.9574	1.685	1.886	0.00017	0.4596	2	0.004	34.8	178.1
0.8511	1.498	1.676	0.00015	0.4088	1	0.000	39.0	205.0
0.7447	1.311	1.467	0.00013	0.3571	0	0.000	44.3	205.5
0.6383	1.123	1.257	0.00011	0.3069	0	0.000	51.8	215.1
0.5319	0.936	1.048	0.00010	0.2558	1	0.000	62.2	242.0
0.4255	0.749	0.838	0.00008	0.2045	0	0.000	77.5	263.5
0.3191	0.562	0.629	0.00006	0.1538	0	0.000	104.7	307.0
0.2128	0.374	0.419	0.00004	0.1024	0	0.000	154.2	381.8
0.1064	0.187	0.210	0.00002	0.0507	0	0.000	311.6	527.8
0.0532	0.094	0.105	0.00001	0.0261	0	0.000	626.0	726.3

Int./FT = track intersections per fission event
Sides = number of sides of cubic volume intersected by largest cluster (6 indicates full percolation)

Table 5. Parameters for P_∞ estimation using Equations 2 and 3.

Track type	p_c	β	D_c	b
			α/g x 10^{16}	
α 8-chain	0.01298(10)	3.77(12)	2.236(17)	3.74(12)
α 6-chain	0.01610(36)	4.67(71)	2.962(67)	4.62(70)
α no chain	0.0717(14)	5.80(118)	13.57(28)	5.55(116)
			FT/g x 10^{10}	
fission	0.0001736(11)	1.814(46)	9.657(62)	1.815(46)

Numbers in parentheses indicate 95% confidence interval.